International Specialty Conference on Cold-Formed Steel Structures

(1978) - 4th International Specialty Conference on Cold-Formed Steel Structures

Jun 1st, 12:00 AM

Local Buckling of Thin Walled Channels

J. Roorda

K. R. Venkataramaiah

Recommended Citation

LOCAL BUCKLING OF THIN WALLED
CHANNELS

by

K.R. Venkataramaiah[†] and J. Roorda[††]

<u>INTRODUCTION</u>

It is well established [5, 10, 13] that a geometrically
perfect stiffened plate or a thin-walled composite of perfect plates,
subjected to longitudinal compressive forces, remains unbuckled until
the critical load is attained, at which stage it assumes a stable
deflected equilibrium configuration. This interchange between two
stable forms - one flat and another deflected - is characteristic of
plate structures and leads to what is appropriately called a stable
post-local-buckling strength. In practice, the presence of unavoidable
imperfections will cause deflections to grow from first application
of the load; the rate of growth becoming larger as the critical load
is approached [9] . The load-deflection curves for both geometrically
perfect and imperfect plate or plate composites are shown in Figure 1a.

For design purposes, and particularly for establishing the
load factors or the safety factors, the local buckling stress is
useful because it indicates the loading value at which the deflections
are still moderate and the structural elements still have a reserve of
strength. Also near this stress significant deformations are initiated
which eventually lead to the failure of the member. These aspects
are important in engineering applications of thin walled sections.

[†] Senior Engineer, Konforti and McCavour Ltd.
Toronto, Ontario, Canada

[††] Professor, Dept. of Civil Engineering,
University of Waterloo, Waterloo, Ontario, Canada

The problem of local buckling of thin-walled sections under concentric compression has been studied by a number of investigators in the past [2, 3, 6, 8, 11, 14, 17 and 26]. However, the case of eccentric compression has received relatively little attention. In this paper, the elastic local instability characteristics of thin-walled channel sections subjected to eccentric compression is considered, the eccentricity being in the plane of symmetry. The loaded edges are considered to be simply supported. The following unloaded edge conditions of plates commonly used in engineering designs are thought to be relevant: (i) Both unloaded edges are elastically restrained as in web-flange junctions; (ii) One edge is elastically restrained as in (i), and the other is simply supported; (iii) One edge is elastically restrained as in (i), and the other elastically built in, due to an edge stiffener for example.

Unloaded edge condition (i) relates to the web component, and conditions (ii) and (iii) are concerned with flange components of the stiffened channel section (shown in Figure 2). For determining the local buckling stresses the exact solution is used for web buckling and the Galerkin method is utilized for flange buckling. The method presented here makes no attempt to calculate explicitly the edge restraints imposed by adjacent plates on each other. Such an attempt would be very difficult. The theoretical analysis of finding critical stresses of channel sections was, however, done by determining the stiffnesses of the web and flange elements at their common edge, and by using the criterion of vanishing combined stiffness at this edge. The solution is one of trial and error. The extensive computations involved necessitated the use of a computer. All such computations were carried out on the IBM 360/75 computer at the University of Waterloo.

RELATED PREVIOUS WORK

Analysis of a thin-walled member such as a channel section as a unit is very complex. Therefore, one of the important simplifications made from a theoretical viewpoint is to consider a thin-walled member as a composite of individual plate components. The load bearing or behavioural properties of individual components are obtained and using these properties compatible conditions along the common adjoining edges are sought. First, the work related to individual plates will be discussed.

The fundamental differential (equilibrium) equation for the deflection, w, of a plate subjected to forces in its middle plane (Figure 1b) under ideal conditions, was first derived by St. Venant [22] in 1883 as follows:

$$\frac{\partial^4 w}{\partial x^4} + 2\frac{\partial^4 w}{\partial x^2 \partial y^2} + \frac{\partial^4 w}{\partial y^4} = \frac{t}{D}\left(\sigma_{xx}\frac{\partial^2 w}{\partial x^2} + 2\tau_{xy}\frac{\partial^2 w}{\partial x \partial y} + \sigma_{yy}\frac{\partial^2 w}{\partial y^2}\right) \qquad (1)$$

where σ_{xx} = normal stress in x-direction, σ_{yy} = normal stress in y-direction, τ_{xy} = shear stress in a section perpendicular to the plane cut parallel to the x- or y-axis, t = plate thickness, and $D = Et^3/12\,(1-\nu^2)$, the flexural rigidity of the plate in which E = modulus of elasticity, and ν = Poission's ratio of the plate material. Equation (1) is based on small deflection theory. If the loading is uni-axial (Figure 1c), then $\sigma_{yy} = 0$ and $\tau_{xy} = 0$. Equation (1) then assumes the simplified form

$$\frac{\partial^4 w}{\partial x^4} + 2\frac{\partial^4 w}{\partial x^2 \partial y^2} + \frac{\partial^4 w}{\partial y^4} = -\frac{t}{D}\sigma_{xx}\frac{\partial^2 w}{\partial x^2} \qquad (2)$$

Birfucation of the equilibrium position is indicated by the lowest characteristic value of the parameter σ_{xx} in Equation (2), called the critical stress or the local buckling stress, σ_{cr}. In 1890 Bryan

[5] presented the analysis for the rectangular plate, simply supported on all its four edges and subjected to uniform compression on two edges (Figure 1c). For this case, σ_{cr} can be derived from Equation (2) as

$$\sigma_{cr} = k \frac{\pi^2 E}{12(1-\nu^2)\ (b/t)^2} \tag{3}$$

where b/t = thinness ratio of the plate, and k = local buckling constant which depends upon the aspect ratio of the plate and the manner in which it is supported, chiefly along the longitudinal edges parallel to the compressive forces. For long narrow plates (that is, with an aspect ratio ≥ 4) k can be assumed to be equal to a constant value of 4 when the unloaded edges are simply supported. When these edges are fixed, k reaches a value of 6.97 [3] . In the case of plate components, such as the web in Figure 2, the value of k lies between 4 and 6.97 due to the presence of mutual restraint at the longitudinal junctions of the plate components.

A fundamental approach to the problem of instability of cross-sections composed of a number of plate elements is due to Lundquist [20]. In this reference the local instability of a plain channel has been studied. A stiffness criterion was developed to determine the lowest critical stress and the corresponding mode of buckling. When two or more plate elements join along an edge which is parallel to the longitudinal axis of a plate composite, that value of longitudinal stress at which the algebraic sum of stiffness of the individual plate elements vanishes is the critical stress for the plate composite. The stiffnesses referred to above are defined as the moments per unit length along the longitudinal axis required to produce a transverse rotation of a quarter of a radian at the common edge. In order

to use this method, the local buckling constants, k, must be known
as functions of the edge restraint, c, and the half wave length of
buckle, λ, for all loaded plates in the system. Lundquist and
Stowell have published charts for the critical stresses of outstanding
flanges [19] and for long plates with equal and opposite restraints
on unloaded edges [18]. Tables for stiffnesses and carry-over factors
for rectangular plates under compression are given by Kroll [16].
Van der Maas [26] has presented critical stress charts for local
instability of columns with "hat" sections.

The solution to the problem of a single plate under compression
and bending in its plane has been obtained by Schuette and McCulloch
[23] who have also published charts for such cases. Johnson and Noel
[15] have published charts for plates subjected to bending in their
own plane, for four positions of the axis of zero stress. Johnson and
Noel suggest that their results should be used in combination with
tables published by Kroll [16] in order to arrive at buckling loads
for sections under eccentrically applied loading.

Walker [27] has studied plates and channel sections subjected
to eccentric compression by means of an approximate solution using the
Galerkin method. According to Walker - "Instability occurs in the
section as a whole; that is, the individual plates each become
unstable simultaneously at the particular load considered and for the
relevant mutual boundary conditions. Thus, by using approximate
geometrical procedure the flange plates can be matched to a given web
plate so that the load at which the assembly of plates becomes unstable
as a unit is obtained".

In engineering designs of thin-walled sections, it is not uncommon for the resultant load to be either offset from the centroid or combined with an applied moment so that non-uniform stresses are set up across the widths of some or all individual plate components. Rhodes and Harvey [21] utilized the principle of minimum potential energy to obtain the local buckling stresses of plain channels under combined compression and bending, in which the edges of outstanding flanges were free. The analysis has been extended to lipped and trapezoidal sections with an assumption that the lip-flange junctions satisfy the simply supported condition. The buckled half wave length that gives the lowest possible buckling stress was evaluated by inspection of the eigen values obtained for a number of values of the half wave length.

MATHEMATICAL FORMULATION

Figure 2a shows a thin-walled member subjected to an eccentric load, P, in the plane of symmetry. It is assumed that the load acts on the ends of the member through rigid plates which prevent warping of the end plane. The eccentric force on the section can be replaced by the equivalent stress system on the individual plate components as shown in Figure 2b. In Figure 2c are shown the free body diagrams of the flange and the web plates. Although only the straight-lip edge stiffener is shown in Figure 2, stiffeners of other shapes can be considered in a similar way.

With reference to Figure 2, the longitudinal axis of the column is taken as the X-axis, and the transverse direction in the plane of the web or flange, as applicable, is taken as the Y-axis.

The Z-axis defines the out-of-plane deformations of the plate elements. Since the deformations within the thickness of the plate are not considered, the relevant functions are all independent of Z-coordinates.

The edge moments at the root of the outstanding flange, and at the unloaded edges of the web are assumed to vary sinusoidally along the length of the channel. The buckled surface of the plate components is assumed to be defined by the following equation:

$$w = \sin \frac{\pi x}{\lambda} f(y) \tag{4}$$

where $\lambda = \ell/m$, in which $\ell =$ length of the plate and $m =$ an integer. The above assumption implies that consideration of the plate in any one half wave (Figure 2c) would apply equally to any other half wave along the length of the member. It has been observed in tests that Equation (4) represents reasonably well the deformed surface of a long plate in the regions remote from the end restraints.

By choosing the stress on the web plate for reference, the stress distribution on the flange plate can be described as

$$\sigma_{xx} = \sigma_o [(1-\gamma/2) - \gamma \frac{y}{b_f}] \tag{5}$$

where $\sigma_o =$ reference stress on the web plate, $\gamma =$ load eccentricity parameter, $y =$ co-ordinate in Y-direction, and $b_f =$ width of flange. The magnitude of σ_o that causes local buckling of the section is now sought.

In setting up the appropriate boundary conditions which would allow an exact solution of equation (2) for the web, or an approximate solution for the flange because of the variation in loading condition, the following assumptions have been made:

(i)   The longitudinal edge at the root of the flange remains
      straight throughout the process of loading, not undergoing
      any deflection either in Y or Z direction [20].

(ii) The flange and web plates are assumed to buckle with the
      same wavelength, 2λ, with buckles remaining in phase
      throughout.

(iii) The restraining moment applied by the web plate on the
      flange at the common edge, or vice versa, is assumed to
      vary sinusoidally along the length, that is in X-direction.

(iv) At every station along the length of the plate the moment
      'M' along the edge and the rotation 'θ' in the YZ plane
      bear a constant linear relationship to each other and the
      ratio M/θ is independent of the X-co-ordinate [3 and 24].

The analyses of the web and the flange plate components are now
presented separately.

WEB PLATE WITH UNIFORM COMPRESSION ON LOADED EDGES AND EQUAL AND OPPOSITE MOMENTS APPLIED ALONG THE UNLOADED EDGES

With reference to the web plate shown in Figure 2c, $\sigma_{xx} = \sigma_o$. Equation (2), as applied to the web plate, can be written as:

$$\frac{\partial^4 w}{\partial x^4} + \frac{2\partial^4 w}{\partial x^2 \partial y^2} + \frac{\partial^4 w}{\partial y^4} + \frac{\pi^2 k_w}{b_w^2}\frac{\partial^2 w}{\partial x^2} = 0 \tag{6}$$

where b_w = web width, and $k_w = \dfrac{\sigma_o b_w^2 t}{\pi^2 D}$ (k_w is the web buckling

constant). Substitution of equation (4) in equation (6) yields the
following differential equation for $f(y)$:

$$\frac{d^4 f(y)}{dy^4} - \frac{2\pi^2}{\lambda^2}\frac{d^2 f(y)}{dy^2} + (\frac{\pi^4}{\lambda^4} - \frac{\pi^4 k_w}{b_w^2 \lambda}) f(y) = 0 \tag{7}$$

The general solution of this ordinary differential equation is of the form

$$f(y) = c_1 \cosh \frac{\alpha y}{b_w} + c_2 \sinh \frac{\alpha y}{b_w} + c_3 \cos \frac{\beta y}{b_w} + c_4 \sin \frac{\beta y}{b_w} \qquad (8)$$

where c_1, c_2, c_3, and c_4 are constants that depend upon boundary conditions along the edges $y = \pm\, b_w/2$, and

$$\alpha = \pi \sqrt{\frac{b_w}{\lambda}} \sqrt{\frac{b_w}{\lambda} + \sqrt{k_w}} \qquad (9a)$$

$$\beta = \pi \sqrt{\frac{b_w}{\lambda}} \sqrt{-\frac{b_w}{\lambda} + \sqrt{k_w}} \qquad (9b)$$

Equation (4), with $f(y)$ given by equation (8), should satisfy the following two unloaded edge boundary conditions:

$$(w)_{y = \pm\, b_w/2} = 0 \qquad (10a)$$

$$-D \left(\frac{\partial^2 w}{\partial y^2} + \nu \frac{\partial^2 w}{\partial x^2}\right)_{y = \pm\, b_w/2} = M = M_o \sin \frac{\pi x}{\lambda} \qquad (10b)$$

where M_o is the amplitude of sinusoidally distributed moment, M. According to the sign convention used (see Figures 2 and 3), the moment is positive if it produces out-of-plane deflection in the direction of the moment. Thus the moments at the two edges have the same sign although they act in opposite directions.

The magnitude of "M" itself is not determined from the differential equation and the conditions at the boundary. This, however, is inconsequential since the stiffness M/θ is constant, where θ is the rotation along the edge $y = b_w/2$ for example, expressed

in radians. In the sequel, stiffness is defined as the moment per unit length along the longitudinal axis required to produce a transverse rotation of one radian at the edge at which all plate elements join. The stiffness of the web may then be written as

$$S_w = \left(\frac{M}{\theta}\right)_y = b_w/2 \tag{11}$$

where

$$(\theta)_y = b_w/2 = \left(\frac{\partial w}{\partial y}\right)_y = b_w/2 \tag{12}$$

By means of the boundary conditions given by equations (10a) and (10b), the arbitrary constants in equation (8) may be computed, and the deflection surface for the web plate thus determined. From the deflection surface, the rotation θ can be found from equation (12). Substitution of the expression for θ in equation (11) results in the following expression for the stiffness of the web plate:

$$S_w = \frac{D}{b_w} \frac{[(\frac{\alpha}{2})^2 + (\frac{\beta}{2})^2]}{[\frac{\alpha}{2}\tanh\frac{\alpha}{2} + \frac{\beta}{2}\tan\frac{\beta}{2}]} \tag{13}$$

STIFFENED FLANGE PLATE SUBJECTED TO NON-UNIFORM COMPRESSION ON LOADED EDGES

Considering the flange plate shown in Figure 2c, the following equilibrium equation, which is a combination of equations (2) and (5) may be derived:

$$\frac{\partial^4 w}{\partial x^4} + \frac{2\partial^4 w}{\partial x^2 \partial y^2} + \frac{\partial^4 w}{\partial y^4} = -\frac{\pi^2 k_f}{b_f^2}\left[(1 - \frac{y}{2}) - \frac{yy}{b_f}\right]\frac{\partial^2 w}{\partial x^2} \tag{14}$$

where

$$k_f = \frac{\sigma_o b_f^2 t}{\pi^2 D} \quad (k_f \text{ is the flange buckling constant}).$$

Equation (14) is transformed into non-dimensional form with

$$\xi = \frac{x}{t}, \quad \eta = \frac{y}{b_f}, \quad \phi = \frac{t}{b_f}, \quad \text{and} \quad \omega = \frac{w}{t};$$

where ℓ is the length of the plate in the X-direction. Equation (14) then takes the form

$$\frac{1}{\phi^2}\frac{\partial^4\omega}{\partial\xi^4} + \frac{2\partial^4\omega}{\partial\xi^2\partial\eta^2} + \phi^2\frac{\partial^4\omega}{\partial\eta^4} = -\pi^2 k_f \left[(1-\frac{\gamma}{2}) - \gamma\eta\right]\frac{\partial^2\omega}{\partial\xi^2} \qquad (15)$$

The solution of (15) may be assumed as

$$\omega = f(\xi)\, g(\eta) \qquad (16)$$

It is impossible to get an exact solution of (15). Therefore, an approximate solution is attempted by using the Galerkin [12] method. The functions $f(\xi)$ and $g(\eta)$ should be such that they satisfy the boundary conditions and also lend themselves to the use of the Galerkin method. The boundary conditions of the loaded edges, which are considered to be simply supported, are (in dimensionless form):

$$[\omega]_{\xi=0,1} = 0 \qquad (17a)$$

and

$$\left[\frac{\partial^2\omega}{\partial\xi^2} + \nu\phi^2\frac{\partial^2\omega}{\partial\eta^2}\right]_{\xi=0,1} = 0 \qquad (17b)$$

The function $f(\xi)$ may be taken as

$$f(\xi) = \sin m\pi\xi, \quad (m = 1,2,3, \ldots) \qquad (18)$$

Substitution of equations (16) and (18) into (15) results in

$$\frac{d^4 g(\eta)}{d\eta^4} - \frac{2m^2\pi^2}{\phi^2}\frac{d^2 g(\eta)}{d\eta^2} + \frac{m^4\pi^4}{\phi^4} g(\eta) = \frac{k_f m^2\pi^4}{\phi^2}\left[(1-\frac{\gamma}{2})-\gamma\eta\right]g(\eta) \qquad (19)$$

The eigen values k_f of equation (19) subject to the relevant unloaded edge boundary conditions, are now sought. The function $g(\eta)$ is taken in the polynomial form

$$g(\eta) = q_n g_n(\eta); \quad n = 0,1,2,3, \ldots, \qquad (20)$$

where

$$g_n(\eta) = \eta^{n+4} + A_n \eta^{n+3} + B_n \eta^{n+2} + C_n \eta^{n+1} + D_n \eta^n$$

$$n = 0,1,2,3, \ldots \qquad (21)$$

A_n, B_n, C_n and D_n have to be determined on the basis of the unloaded edge boundary conditions. The stiffened flange plate is analyzed for two different conditions at the flange-stiffener junctions - (i) the simply supported condition and (ii) the elastically built in condition.

FLANGE PLATE COMPONENT ELASTICALLY RESTRAINED BY WEB ON ONE UNLOADED EDGE AND SIMPLY SUPPORTED (BY A STIFFENER) AT THE OTHER EDGE

Considering Figure 2c and assuming simply supported edge conditions at the flange-stiffener junction, the boundary conditions at $y = \pm b_f/2$ ($\eta = \pm 1/2$) may be written as

$$[\omega]_{\eta = -1/2} = 0 \qquad (22a)$$

$$[\omega]_{\eta = +1/2} = 0 \qquad (22b)$$

$$\left(\frac{\partial^2 \omega}{\partial \eta^2} + \frac{\nu}{\phi^2} \frac{\partial^2 \omega}{\partial \xi^2}\right)_{\eta = -1/2} = r_f \left(\frac{\partial \omega}{\partial \eta}\right)_{\eta = -1/2} \qquad (23a)$$

and

$$\left(\frac{\partial^2 \omega}{\partial \eta^2} + \frac{\nu}{\phi^2} \frac{\partial^2 \omega}{\partial \xi^2}\right)_{\eta = +1/2} = 0 \qquad (23b)$$

where $r_f = -\dfrac{S_f b_f}{D}$ is called the elastic rotational restraint coefficient and is the non-dimensional form of stiffness per unit length in X-direction at the root of the flange.

Application of these boundary conditions to the deflection surface prescribed by equations (16), (18) and (20) leads to

$$
\begin{bmatrix}
2 & -4 & 8 & -16 \\
2 & 4 & 8 & 16 \\
2(n+3)\left[(n+2)+\dfrac{r_f}{2}\right] & -4(n+2)\left[(n+1)+\dfrac{r_f}{2}\right] & 8(n+1)\left[n+\dfrac{r_f}{2}\right] & -16n\left[(n-1)+\dfrac{r_f}{2}\right] \\
2(n+3)(n+2) & 4(n+2)(n+1) & 8(n+1)n & 16n(n-1)
\end{bmatrix}
\begin{bmatrix}
A_n \\ B_n \\ C_n \\ D_n
\end{bmatrix}
$$

$$
=
\begin{bmatrix}
1 \\
-1 \\
(n+4)\left[(n+3)+\dfrac{r_f}{2}\right] \\
-(n+4)(n+3)
\end{bmatrix}
\tag{24}
$$

Constants A_n, B_n, C_n and D_n can be determined from equation (24) in its matrix form for assigned values of n and r_f.

FLANGE PLATE COMPONENT ELASTICALLY RESTRAINED BY A WEB ON ONE EDGE AND ELASTICALLY BUILT IN BY A STIFFENER AT THE OTHER EDGE (SEE FIGURE 3)

The flange is here considered as elastically built in, because the bending moments that appear during buckling along the edge are proportional at each point to the angle of rotation of the edge. The angle of rotation of the stiffener is equal to $\partial w/\partial y$, and the rate of change of this angle is $\partial^2 w/\partial x \partial y$. Hence the twisting moment at any cross-section of the stiffener is $GJ(\partial^2 w/\partial x \partial y)$ where GJ is its torsional rigidity. The warping rigidity of the stiffener is neglected here [11, 24]. The rate of change with respect to x of the twisting moment is numerically equal to the bending moment, M, per unit length along the flange edge $y = + b_f/2$. Because of the equilibrium of the moments at the stiffener-flange junction, the moment on the stiffener will have a sign opposite in sense to the one acting on the edge of the flange. Hence the corresponding boundary condition along the flange-stiffener junction is

$$-D\left(\frac{\partial^2 w}{\partial y^2} + \nu \frac{\partial^2 w}{\partial x^2}\right) = -GJ \frac{\partial^3 w}{\partial x^2 \partial y} \tag{25}$$

Edge stiffeners, particularly narrow ones, can be regarded
as columns buckling under the combined action of an end compressive
stress and lateral shear loading transmitted from the flange plate to
the stiffener (see Figure 3b). During buckling the plate tries to
deflect, but is resisted by the stiffener acting like an elastic beam,
and therefore, bending of the stiffener follows. Referring to Figure 3b,
equilibrium of the junction between the flange and the stiffener exists
if the following conditions are satisfied: (i) the lateral bending of
the flange is equal to the bending of the stiffener in the Z-direction,
and (ii) the shear loading transmitted from flange is resisted by the
stiffener acting like an elastic beam. Equilibrium of moments is
already considered. To consider the bending of the stiffener, it
can be assumed that the uniform compressive force on the stiffener is
equal to $A_s \sigma_s$, where A_s is the cross-sectional area of the stiffener
and σ_s the uniform stress acting on it. Denoting the flexural rigidity
of the stiffener by EI_s, where I_s is the moment of inertia about the
neutral axis of the stiffener, the differential equation of its deflection
curve is

$$EI_s \frac{\partial^4 w}{\partial x^4} = D\left[\frac{\partial^3 w}{\partial y^3} + (2-\nu) \frac{\partial^3 w}{\partial x^2 \partial y}\right] - A_s \sigma_s \frac{\partial^2 w}{\partial x^2} \tag{26}$$

Consequently, the following boundary conditions, in non-dimensional
form, for the flange plate component shown in Figure 3 may be
formulated:

$$[\omega]_{\eta = -1/2} = 0 \tag{27a}$$

$$\left(\frac{\partial^2 \omega}{\partial \eta^2} + \frac{\nu}{\phi^2} \frac{\partial^2 \omega}{\partial \xi^2}\right)_{\eta = -1/2} = r_f \left(\frac{\partial \omega}{\partial \eta}\right)_{\eta = -1/2} \tag{27b}$$

$$\left(\frac{\partial^2 \omega}{\partial \eta^2} + \frac{\nu}{\phi^2} \frac{\partial^2 \omega}{\partial \xi^2}\right)_{\eta = +1/2} = \left(\frac{GJ}{D\phi^2 b_f} \frac{\partial^3 \omega}{\partial \xi^2 \partial \eta}\right)_{\eta = +1/2} \tag{27c}$$

and

$$EI_s \left(\frac{\partial^4 \omega}{\partial \xi^4}\right)_{\eta = +1/2} = D[\phi^3 \ell \frac{\partial^3 \omega}{\partial \eta^3} + (2-\nu)\phi\ell \frac{\partial^3 \omega}{\partial \xi^2 \partial \eta}] -$$

$$A_s \sigma_s \ell^2 \left(\frac{\partial^2 \omega}{\partial \eta^2}\right)_{\eta = +1/2} \tag{27d}$$

The boundary conditions in equations (27a) and (27b) are dependent upon the assumed mode of buckling, the value of M_o and the magnitude of the half wave length of buckle, λ. The boundary conditions in (27c) and (27d) are determined by equilibrium considerations and are independent of the assumed mode. It is not possible to assign known values of M, the moment at any station, and λ, since the geometry of the deformed surface cannot be explicitly stated. Therefore, the solution is arrived at through a trial and error procedure by which the lowest critical longitudinal force and the corresponding buckling mode are found.

The following matrix equation can be derived by applying the boundary conditions given in equations (27a) to (27d) to the deflection surface assumed through equations (16), (18) and (20):

$$
\begin{bmatrix}
2 & -4 \\
2(n+3)[(n+2)+r_f/2] & -4(n+2)[(n+1)+r_f/2] \\
8(n+3)(n+2)-2V+4(n+3)U & 16(n+2)(n+1)-4V+8(n+2)U \\
2V_V+4(n+3)R_R-16(n+3)(n+2)(n+1)U_U & 4V_V+8(n+2)R_R-32(n+2)(n+1)(n)U_U
\end{bmatrix}
$$

$$
\begin{bmatrix}
8 & -16 \\
8(n+1)[n+r_f/2] & -16n[(n-1)+r_f/2] \\
32(n+1)(n)-8V+16(n+1)U & 16n(n-1)-16V+32(n)U \\
8V_V+16(n+1)R_R-64(n+1)n(n-1)U_U & 16V_V+32nR_R-128(n)(n-1)(n-2)U_U
\end{bmatrix}
\begin{bmatrix} A_n \\ B_n \\ C_n \\ D_n \end{bmatrix}
$$

$$
=
\begin{bmatrix}
1 \\
(n+4)[(n+3)+r_f/2] \\
-[4(n+4)(n+3)-V+2(n+4)U] \\
-[V_V+2(n+4)R_R-8(n+4)(n+3)(n+2)U_U]
\end{bmatrix}, \quad (28)
$$

where $\quad R = \dfrac{m^4\pi^4}{\phi^4}, \quad R_R = (2-\nu)Db_f \dfrac{m^2\pi^2}{\phi^2},$

$$
V = \frac{m^2\pi^2}{\phi^2}\nu, \quad V_V = EI_s \frac{m^4\pi^4}{\phi^4} - A_s\sigma_s\, b_f^2\, \frac{m^2\pi^2}{\phi^2}
$$

$$
U = \frac{GJ}{Db_f}\, \frac{m^2\pi^2}{\phi^2}, \quad \text{and} \quad U_U = Db_f
$$

The constants A_n, B_n, C_n and D_n can be found from equation (28) for
assigned values of n, r_f, loading properties, and the edge stiffener
geometry. By assigning zero dimensions for the edge stiffener in
equation (28) the resulting matrix equation coincides with the one
derived for the plain channel by Walker [27].

EVALUATION OF THE FLANGE BUCKLING CONSTANT

The solution to equation (19) may be formulated using Galerkin's method as

$$\int_{-1/2}^{1/2} \{\frac{d^4 g(\eta)}{d\eta^4} - 2 \frac{m^2 \pi^2}{\phi^2} \frac{d^2 g(\eta)}{d\eta^2} + \frac{m^4 \pi^4}{\phi^4} g(\eta) - k_f \frac{m^2 \pi^4}{\phi^2} [(1 - \frac{\gamma}{2}) - \gamma\eta] g(\eta)\} \frac{\partial g(\eta)}{\partial q_n} d\eta$$

$$= 0 \qquad (29)$$

Equations (20) and (21) are used to define $g(\eta)$, in which the constants A_n, B_n, C_n and D_n have to be found by using the boundary conditions given in the form of matrix equation (24) or (28). The solution is obtained by expanding equation (29). Use of equations (20) and (21) yields Galerkin equations of the form

$$\sum_{n = 0,1,2,\ldots,L} q_n \int_{1/2}^{1/2} \{\frac{d^4 g_n(\eta)}{d\eta^4} - 2 \frac{m^2 \pi^2}{\phi^2} \frac{d^4 g_n(\eta)}{d\eta^2} + \frac{m^4 \pi^4}{\phi^4} g_n(\eta)$$

$$- k_f \frac{m^2 \pi^4}{\phi^2} [(1 - \frac{\gamma}{2}) - \gamma\eta] g_n(\eta)\} g_j(\eta) d\eta = 0 \qquad (30)$$

$$j = 1,2,3,\ldots,L.$$

L indicates the limit of the number of terms included in the Galerkin series. Then the following square matrix of the coefficients q_n may be constructed as:

$$\begin{bmatrix} (M_{00} - k_f N_{00}) & (M_{01} - k_f N_{01}) & \cdots & (M_{0L} - k_f N_{0L}) \\ (M_{10} - k_f N_{10}) & (M_{11} - k_f N_{11}) & \cdots & \cdots \\ \cdot & & & \\ \cdot & & & \\ \cdot & & & \\ (M_{L0} - k_f N_{L0}) & \cdots & \cdots & (M_{LL} - k_f N_{LL}) \end{bmatrix} \begin{bmatrix} q_0 \\ q_1 \\ \cdot \\ \cdot \\ \cdot \\ q_L \end{bmatrix} = 0 \qquad (31)$$

A typical element of the above matrix is given in the Appendix.

The values of k_f have practical meaning only for the non-trivial values of q_n. This means that values of k_f for which the determinant of the matrix in equation (31) is zero have to be found. The only value of relevance in this investigation is the lowest real one. Of the many methods available for the determination of k_f, the method of solving simultaneous equations by Gaussian elimination with pivotal condensation was used in this investigation. This necessitated the employment of a "trial and error" type procedure. The large number of computations involved were practicable only with the use of a computer.

LOCAL BUCKLING STRESSES OF CHANNEL SECTIONS

For the channel section shown in Figure 2, both the loading and sectional geometry have the same plane of symmetry. This symmetry can be utilized in the local instability analysis. The web plate may be treated as the reference plate and the plane of symmetry can be used as a boundary for the half section where necessary. The theoretical analysis of the channel section is done by means of the expression for stiffness (13) of the web plate component at the web-flange junction and by using the criterion of vanishing stiffness (i.e., $S_w + S_f = 0$) at this junction.

Consider the common edge where a flange and a web plate meet. At this edge there is a certain magnitude of bending moment transmitted from the web to the flange and vice versa at every station along the length of the junction. If the flange is considered alone without the web, it is possible to introduce a restraining sinusoidal moment along the common edge as an external moment. Similarly for the web, the moments transmitted by the two flanges can be replaced by sinusoidally

varying bending moments of the same sign acting along the opposite edges
of the web plate. A treatment of the plate composite in this manner
makes it possible to consider an external moment acting on the web-flange
junction. If an external moment is assumed to act on this junction, the
rotation of the junction would depend upon the algebraic sum of stiffnesses
supplied by the web and flange elements against flexure. These stiffnesses
decrease with the longitudinal stress at varying rates depending upon the
individual and the relative web and flange geometries and the nature of
the edge restraints. The weaker of the two elements reaches a zero
stiffness at some longitudinal stress and begins to develop negative
stiffness. That is, the weaker element then requires restraint from an
adjoining stronger element in order to sustain further stress without
itself succumbing to premature local buckling. This negative stiffness
tends to supplant the positive stiffness of the other elements meeting at
an edge until the sum of all stiffnesses become zero. When this happens,
large joint rotations occur. This is the condition which defines the
critical stress on the section.

For a particular axial stress defined by the buckling constant,
k, and a particular mode of buckling specified by a specific half wave
length, the web-flange junction stiffness can be numerically computed.
By keeping the half wave length constant and trying several values of
longitudinal stress the one satisfying the "vanishing stiffness criterion"
can be found. Then, varying the length of half wave of buckle, the
corresponding values of stress meeting the same criterion are computed.
Considering all these values of stress and the corresponding modes, it
is possible to determine the minimum value of stress (i.e., critical
stress) and the corresponding mode of buckling. This procedure not

only yields the critical stress, but also defines the mode of buckling (i.e., half wave length, λ).

The following relationships are true at the web-flange junction when it reaches the vanishing stiffness condition:

$$S_f + S_w = 0 \tag{32}$$

By definition

$$r_f = - \frac{S_f b_f}{D}; \; r_w = - \frac{S_w b_w}{D}, \tag{33}$$

where r_w is related to the web with the same definition as for r_f. Therefore

$$r_f = \frac{S_w b_f}{D}, \tag{34}$$

also

$$k_w = \frac{k_f}{(b_f/b_w)^2} \tag{35}$$

COMPUTATIONAL PROCEDURES

The computations can be based on choosing values for either "k_w" or "k_f", since the critical value of each of these quantities yields the same value for critical stress on the basis of the vanishing stiffness criterion. The computations in the present investigation were based on "k_f". Certain values of "k" were assumed as bounds in the computation. For example, "k_w" was assumed never to exceed 7, which is the value for a uniformly loaded plate with fixed unloaded edges. The Poisson's ratio for elastic calculations was taken as 0.3. The shear modulus was assumed to be 11,300 ksi (77911MN/m^2).

The procedure followed in the computer programme to determine the critical stress on the basis of the vanishing stiffness criterion

is outlined here in the point form.

1. A half wave length of buckle "λ" is assumed.

2. A value for the buckling constant "k_f", corresponding to a trial value of longitudinal stress, is selected and hence "k_w" is determined (Eq. 35).

3. "S_w" is computed (Eq. 13) and hence "r_f" (Eq. 34).

4. A_n, B_n, C_n and D_n are determined (Eq. 24 or Eq. 28).

5. The determinant of the matrix in Eq. (31) is calculated.

6. If this determinant is not zero, a different value of "k_f" is assumed and steps 2 through 6 are repeated until the determinant vanishes.

7. The entire procedure, steps 1 through 6, is repeated for other values of half wave length "λ" until a sufficiently accurate global minimum value of "k_f" is obtained.

8. The critical load or stress is that which corresponds to the minimum "k_f" determined in 7 above, and the value of "λ" for which "k_f" is a minimum is the critical half wave length and hence the mode of buckling for the particular section geometry.

The solution obtained by the use of Galerkin series seems to be rapidly convergent. The solutions for the flange buckling constant, k_f, and the corresponding mode of buckling indicated by the half wave length of the buckle for increasing numbers of terms, are given in Table 1. The table includes values for:

(a) channel sections with different shapes of edge stiffeners;

(b) four different cases of concentric or eccentric

loadings varying from uniformly compressed to pure
bending, and

(c) the flange-stiffener junction treated as simply
supported (Eq. 24) and elastically built in conditions
(Eq. 28).

It is evident from Table 1 that three terms in the Galerkin series
result in a solution with a degree of convergence sufficient for
engineering purposes. In the final computations, therefore, only
three terms were included.

CHANNEL SECTIONS INVESTIGATED

The channel geometries shown in Fig. 4a were analyzed to
determine the elastic critical stress under concentric loading. The
overall nominal cross-sectional dimensions of the channels in Series B,
MCM, T1LL, T2LL, T3LL, T4LL and MCMC were 8 by 4 inches (203 by 102 mm).
For series CSLL these dimensions were 6 by 2 1/4 inches (152 by 57 mm).
Series G20CS, G20TS, G22CS, G22TS and G24CS had overall cross-sectional
dimensions of 8 by 3 inches (203 by 76 mm). The relevant dimensions
of the edge stiffeners in the latter five series were in accordance
with the provisions of Refs. [1] and [7] (Note: the edge stiffener
provisions of the revised 1974 CSA Standard are very close to those
contained in the 1963 CSA Standard). Series D, E and H were nominally
4 x 1 13/16 inches (102 by 46 mm). The straight lip stiffener is
Series H was designed according to the recommendations contained in
[1] and [7].

A listing of the above channels is contained in Table 2.
The corresponding flange thinness ratios are also listed and are based

on exact measurements taken from actual test specimens. A range of b_f/t from 56.3 to 155 is represented by these channels. Computations were done on the basis of the flange-stiffener junction separately satisfying (i) the simple support condition, and (ii) the elastically built in condition.

The cross-sectional shapes analyzed under eccentric loading are shown in Fig. 4b and include Series G8SL, G10SL, G12SL, G14SL, G16LL, G18LL, G20LL, G22LL, G24LL, G26LL, G28LL and G30LL. The provisions of Refs. [1] and [7] formed the basis for the dimensions of the edge stiffener in these series. The flange thinness ratios in these sections ranged from 17.6 to 211.2. The overall nominal cross-sectional dimensions of these series were 8 by 3 inches (203 by 76 mm).

A listing of these channels is contained in Table 3 along with the corresponding flange thinness ratios which are, as before, based on exact measurements taken from real test specimens. Critical stress calculations for both the simply supported and the elastically built in flange-stiffener junction condition were made here also.

The reference stress σ_0 due to eccentric load P - the eccentricity being in the plane of symmetry - can be described as

$$\sigma_{OSL} = \frac{P}{t(b_w+h_f)}, \quad \sigma_{OLL} = \frac{P}{t(b_w+b_f + b_{u\ell}^2/h_f)} \quad (36)$$

where σ_{OSL} = reference stress on web of a straight-lipped channel, and σ_{OLL} = reference stress on web of an L-lipped channel. For the purpose of Eq. (26) or (27d) and to evaluate (28), the axial compressive force on the edge stiffeners can be shown to be

$$P_{SLS} = A_{SLS} \; \sigma_{OSL} (1-\gamma) \qquad\qquad (37)$$

$$P_{LLS} = A_{LLS} \; \sigma_{OLL} \; \frac{[b_{s\ell}(1-\gamma) + b_{u\ell}(1-\gamma + \frac{b_{u\ell}}{2b_f}\gamma)]}{(b_{s\ell} + b_{u\ell})} \qquad (38)$$

where P_{SLS} = axial compressive force on the straight-lipped stiffener, P_{LLS} = axial compressive force on the L-lipped stiffener, A_{SLS} = area of straight-lipped stiffener, A_{LLS} = area of L-lipped stiffener, $b_{u\ell}$ = width of unstiffened lip (Figure 4b), and $b_{s\ell}$ = width of stiffened lip (Figure 4b).

THEORETICAL RESULTS

Figure 5 shows the dependence of the local buckling constants, k_f and k_w, upon the overall geometry, represented by the flange to web width ratio, for concentric and for various eccentricities of loading. In the relevant computations E is taken as 30,000 ksi (206842 MN/m^2). Here the flange-stiffener junction is considered to satisfy simple support conditions as described in Equations (22), (23) and (24). In the course of the computations, the stiffnesses of the web and the flange plates were obtained separately. From these results it was possible to identify which of the two plate components (web or flange) of the channel was the first to develop a negative stiffness.

A series of flange width to web width ratios, b_f/b_w, ranging from 0.4 to 1.4 was chosen for this study. At each specific loading condition, the web width was kept constant and the flange width was varied. It is evident from Fig. 5 that a change in the eccentricity of loading has an insignificant effect on the critical stress of channels

whose b_f/b_w ratios vary from about 0.4 to 0.7. It can also be concluded that an eccentricity towards the web (i.e. $\gamma > 0$) causes both web and flange elements to become stiffer than in the uniformly compressed case ($\gamma = 0$).

In Figure 5, the b_f/b_w ratio beyond which the flange instead of the web becomes the critical element, has been marked with an open circle on each of the k_f-curves and with a black dot on each of the k_w-curves. At these b_f/b_w transition ratios, both elements reach the zero stiffness condition simultaneously. It is of interest to note that both the curves for k_f and k_w obtained for the condition of concentric compression, $\gamma = 0$, show a value of 4 for the b_f/b_w ratio of 1. This value is identical to the buckling constant of a component of a tube with a square cross-section in which case the unloaded edges of each plate component are simply supported. Thus the theory is fairly confirmed.

Column (3) in Tables 2 and 3 give the computed ratios of the flange buckling constants (k_f) based on (i) the elastically built-in condition (numerator), and (ii) the simple support condition (denominator). Calculations were done on actual test specimens. Hence the variations in the results for a specific series are mostly due to, and reflect the usual variation present in, the actual stiffener dimensions that are likely to occur through standard fabricating methods. It is notable from these results that the large majority of specimens with stiffeners designed according to Refs. [1] and [7] do not quite meet the simply supported condition at their flange-stiffener junctions. Although the numerical difference between the ratios obtained (< 1.000) and the

desired ratio (=1.000) is in most cases very small, one may expect a
pronounced difference in the corresponding behaviours and ultimate
load carrying capacity. If the ratio is less than 1.000 the edge
stiffener does not provide enough rigidity to prevent laterally inward
or outward deflection of the flange-stiffener junction in an Euler mode.
Such Euler type behaviour will in turn force the flanges to follow a
similar mode of buckling. A well defined pattern of local buckling in
the web will hence not occur, particularly in the advanced stages of
deformation. Therefore, one may expect a significantly lower ultimate
failure load. Tests on the measured specimens (to be reported elsewhere)
confirm this.

It is appropriate to note here that the computed half wave
lengths of the initial buckling pattern at the critical stress, taken
as a fraction of the web width, varied between 0.78 and 0.82. The
critical stress, however, is relatively insensitive to small changes
in half-wave lengths.

In Figure 6 the computed web buckling constants, k_w, for
channels shown in Figure 4b and reported in Table 3, are plotted against
the corresponding web thinness ratios, $b_{w/t}$. These k_w values were
calculated on the basis of equation (28), which accounts for the actual
boundary conditions at the flange-stiffener junctions of the channels.
The figure demonstrates that the value of local buckling constant for
a uniformly compressed plate component having elastic restraints at its
unloaded edges - the restraint being of intermediate range between
fixed and simply supported edge conditions - is significantly greater
than 4. Winter [28] assumed a value of 4 for such plate components to

derive the effective width formulae contained in Ref. [1]. It appears that this assumption is substantially on the conservative side. A straight line fit to the results given in Figure 6 indicates that a value of 5.6 for k_w provides good agreement with this theoretical data.

In an approximate stability analysis of thin-walled sections, the torsional stiffness, GJ, of the edge stiffeners is usually ignored. Using the present analysis it is possible to study the effect of torsional stiffness on the buckling constant of the stiffened element. In Figures 7 and 8 the computed minimum k_f values are plotted in relation to the size of edge stiffeners as represented by their thinness ratios. Both straight and L-lip stiffeners are considered. In the case of channels with straight lips, the curves at higher values of thinness ratio are shown as dashed lines (Figure 7). Lip sizes in this range could be susceptible to local instability - an aspect not included in the present analysis. Structurally efficient stiffeners should not in themselves be prone to local buckling. Large stiffeners may take the L-lip form shown in Figure 8, which allows an increase in size beyond that of the maximum straight-lip size without becoming subject to local instability. Figures 7 and 8 suggest that the influence of the torsional stiffness of straight-lip and L-lip stiffeners may be neglected in the stability analysis of stiffened channels.

The local buckling stresses of the channel sections presented in Figures 7 and 8 are given in Figures 9 and 10, respectively. These results, and specifically Figure 10, demonstrate that beyond a particular size of edge stiffener, the local buckling stress of the section as a whole does not increase proportionately. This result is useful from

the design point of view. Using the approach presented in these figures,
it is possible to arrive at an optimum size of stiffener for a given.
plate. Thus, a design formula for optimum edge stiffeners suited to
various stiffened plate sizes may be developed. This optimum stiffener
implicitly meets the requirements necessary to provide simple support
conditions at the plate-stiffener junction.

SUMMARY AND CONCLUSIONS

(a) A generalized method of theoretical analysis for the
problem of local buckling of thin-walled channel sections under eccentric
compression is presented. Specific results are obtained for two common
flange-stiffener conditions for which little design information is
available. Plain channels or channels with other flange-stiffener
junctions could also be analyzed in a similar way if appropriate
boundary conditions are substituted.

The criterion for instability used herein states that the
local buckling (critical) stress is attained when the sum of the
transverse stiffnesses of the web and the flange plate components at
their common edge vanishes.

(b) For channels with simple support conditions at their
outstanding flange edges, a family of design curves is developed for
concentric and various eccentric loading arrangements.

(c) The analysis of sections with edge stiffeners designed
on the basis of Canadian and American design code specifications seems
to indicate that the resulting edge stiffeners do not quite meet the
requirements on size necessary to provide the implied simple support

condition at flange-stiffener junctions.

(d) The theoretical half wave length of buckles computed as a fraction of web width is generally around 0.8 for channels whose web widths are greater than their flange widths. Individual cases differ from this value by less than ± 3%.

(e) The local buckling constant of a uniformly compressed plate component having elastic restraints at its unloaded edges, such as the web plate of a channel, was found to be 5.6. This value is substantially greater than the value of 4 assumed for the derivation of the effective width formulae contained in American design specifications.

(f) The influence of the torsional stiffness of straight-lip and L-lip edge stiffeners on the local buckling stress may be neglected in the instability analysis of stiffened sections.

(g) The analysis of stiffened sections suggests that there exists a stiffener size beyond which there is no meaningful increase in the critical stress. By suitable development of this result, a design formula for optimum stiffeners suited to various stiffened plate sizes may be derived.

APPENDIX - REFERENCES

1. American Iron and Steel Institute, "Specification for the Design of Cold-Formed Steel Structural Members", 1968 ed., New York.

2. Becker, H., "Handbook of Structural Stability. Part II - Buckling of Composite Elements", NACA TN 3782, July 1957.

3. Bleich, F., Buckling Strength of Metal Structures, McGraw-Hill Book Co., Inc., New York, 1952.

4. British Standards Institution, "Specification for the Use of Cold-Formed Steel Sections in Building", Addendum No. 1, 1961, to B.S. 449.

5. Bryan, G.H., "On the Stability of a Plane Plate Under Thrusts in its own Plane", Proc. London Math. Soc., Vol. 22, Dec. 1890, pp. 54-67.

6. Bulson, P.S., "Local Instability and Strength of Structural Sections", Thin-Walled Structures, edited by A.H. Chilver, Chatto and Windus, London, England, 1967, pp. 153-207.

7. Canadian Standards Association, "Design of Light Gauge Steel Structural Members", CSA Standard S136-1963, Ottawa, Canada, 1963.

8. Chilver, A.H., "The Stability and Strength of Thin-Walled Steel Struts", The Engineer, 1953, pp. 180-183.

9. Coan, J.M., "Large Deflection Theory for Plates with Small Initial Curvature Loaded in Edge Compression", ASME, Journal of Applied Mechanics, Vol. 18, June 1951, pp. 143-151.

10. Cox, H.L., "Buckling of Thin-Plates in Compression", Technical Report and Memorandum No. 1554, Aeronautical Research Council, London, England, 1933.

11. Divakaran, S., "Local Instability of Thin-Walled Channel Columns with Formed Longitudinal Stiffeners of Circular Cross-section", Ph.D. Thesis, University of Toronto, 1966.

12. Duncan, W.J., "Galerkin's Method in Mechanics and Differential Equations", Technical Reports and Memorandum No. 1798, Aeronautical Research Council, London, England, 1937.

13. Hu, P.C., Lundquist, E.E., and Batdorf, S.B., "Effect of Small Deviations from Flatness on Effective Width and Buckling of Plates in Compression", NACA TN 1124, Sept. 1946.

14. Hu, P.C., and McCulloch, J.C., "The Local Buckling Strength of Lipped Z-Columns with Small Lip Width", NACA TN No. 1335, June 1947.

15. Johnson, J.H., and Noel, R.G., "Critical Bending Stress for Flat Rectangular Plates Supported along all Edges and Elastically Restrained Against Rotation along the Unloaded Compression Edge", Journal of Aeronautical Sciences, Aug. 1953.

16. Kroll, W.D., "Tables of Stiffness and Carry-over Factor for Flat Rectangular Plates under Compression", NACA ARR 3K27, Nov. 1943.

17. Kroll, W.D., Fisher, G.P., and Heimerl, G.P., "Charts for Calculations of Critical Stress for Local Instability of Columns with I, Z, Channel and Rectangular Tube Sections", (NACA Wartime Report L-429), NACA ARR 3K04, Nov. 1943.

18. Lundquist, E.E., and Stowell, E.Z., "Critical Compressive Stress for Flat Rectangular Plates Supported along all Edges and Elastically Restrained against Rotation along Unloaded Edges", NACA Report No. 733, 1942.

19. Lundquist, E.E., and Stowell, E.Z., "Critical Compressive Stress for Outstanding Flanges", NACA Report No. 734, 1942.

20. Lundquist, E.E., Stowell, E.Z., and Schuette, E.H., "Principles of Moment Distribution Applied to Stability of Structures Composed of Bars or Plates", (NACA Wartime Report L-326), NACA ARR 3K06, Nov. 1943.

21. Rhodes, J., and Harvey, J.M., "The Local Instability of Thin-Walled Sections Under Combined Compression and Bending", Third International Specialty Conference on Cold-Formed Steel Structures, University of Missouri-Rolla, Nov. 24-25, 1975.

22. Saint Venant's discussion in "Theorie de l'elasticite des Corps Solides", by Clebsch, final note to Sec. 73, p. 689, 1883.

23. Schuette, E.H., and McCulloch, J.C., "Charts for Minimum Weight Design of Multiweb Wings in Bending", NACA TN No. 1323, June 1947.

24. Timoshenko, S.P. and Gere, M., Theory of Elastic Stability, McGraw-Hill, 1961.

25. Venkataramaiah, K.R., "Thin-Walled Columns", Thesis, University of Waterloo, Waterloo, 1973.

26. VanderMaas, C., "Charts for the Calculation of Critical Compressive Stress for Local Instability of Columns with Hat Sections", Journal of Aeronautical Science, Vol. 21, No. 6, June 1954, pp. 399-403.

27. Walker, A.C., "Local Instability of Thin-Plates and Channel Struts", Journal of the Structural Division, Vol. 92, No. ST3, June 1966, pp. 39-55.

28. Winter, G., "Commentary on 1968 Edition of the Specification for the Design of Cold-formed Steel Structural Members", American Iron and Steel Institute, New York, 1970.

APPENDIX - NOTATION

The following symbols are used in this chapter:

A_n, B_n, C_n, D_n	coefficients in deflection series
A_S	cross-sectional area of stiffener
A_{SLS}	cross-sectional area of straight-lipped stiffener
A_{LLS}	cross-sectional area of L-lipped stiffener
b	width of plate
b/t	thinness ratio of plate
b_f	width of flange plate component
b_w	width of web plate component
$b_{s\ell}$	width of stiffened lip
b_{ul}	width of (unstiffened) lip
C_1, C_2, C_3, C_4	arbitrary constants
D	flexural rigidity of a plate
E	modulus of elasticity
G	shear modulus
GJ	torsional rigidity
I	moment of inertia
I_s	moment of inertia of stiffener
i	integer
J	St. Venant torsion constant
j	integer
k	local buckling constant (coefficient)
k_f	flange buckling constant
k_w	web buckling constat
L	integer
ℓ	length

M	moment along the edge of plate
M_o	amplitude of the sinusoidally distributed moment M
m,n	integers
P	axial load
P_{SLS}	axial compressive force on the straight-lipped stiffener
P_{LLS}	axial compressive force on the L-lipped stiffener
$q_0, q_1, \ldots, q_n$	Galerkin coefficients
r_f	nondimensional elastic rotational restraint of flange
r_w	nondimensional elastic rotational restraint of web
S_f	stiffness of flange
S_w	stiffness of web
t	thickness of plate
w	out-of-plane deflection of plate
x,y,z	co-ordinates in X,Y,Z-axis direction
α, β	parameter in elastic analysis
γ	load eccentricity parameter
ϵ	elastic edge restraint
ξ, η	nondimensional form of Cartesian co-ordinates
ϕ	aspect ratio of plate
θ	rotation
λ	half wave length of buckle
ν	Poisson's ratio of the plate material
σ_{cr}	local buckling (critical) stress
σ_0	reference stress
σ_S	uniform stress acting on the stiffener
σ_{0SL}	reference stress of a straight-lipped channel

σ_{OLL} reference stress of an L-lipped channel

σ_{xx}, σ_{yy} direct stress in X or Y-direction

τ_{xy} shear stress, and

ω nondimensional form of out-of-plane displacement

APPENDIX – A TYPICAL GALERKIN ELEMENT

$$(M_{o2} - k_f N_{o2}) = \{ [(\frac{45}{56} - \frac{5}{192} \frac{m^2 \pi^2}{\phi^2} + \frac{1}{11264} \frac{m^4 \pi^4}{\phi^4}) + B_o (\frac{9}{2} - \frac{15}{112} \frac{m^2 \pi^2}{\phi^2} + \frac{1}{2304} \frac{m^4 \pi^4}{\phi^4})$$

$$+ B_2 (\frac{3}{10} - \frac{3}{56} \frac{m^2 \pi^2}{\phi^2} + \frac{1}{2304} \frac{m^4 \pi^4}{\phi^4}) + D_o (30 - \frac{3}{4} \frac{m^2 \pi^2}{\phi^2} + \frac{1}{448} \frac{m^4 \pi^4}{\phi^4})$$

$$+ D_2 (\frac{1}{448} \frac{m^4 \pi^4}{\phi^4} - \frac{1}{20} \frac{m^2 \pi^2}{\phi^2}) + A_o A_2 (\frac{3}{2} - \frac{5}{56} \frac{m^2 \pi^2}{\phi^2} + \frac{1}{2304} \frac{m^4 \pi^4}{\phi^4})$$

$$+ A_o C_2 (\frac{1}{448} \frac{m^4 \pi^4}{\phi^4} - \frac{3}{20} \frac{m^2 \pi^2}{\phi^2}) + A_2 C_o (10 - \frac{1}{2} \frac{m^2 \pi^2}{\phi^2} + \frac{1}{448} \frac{m^4 \pi^4}{\phi^4})$$

$$+ B_o B_2 (2 - \frac{3}{10} \frac{m^2 \pi^2}{\phi^2} + \frac{1}{448} \frac{m^4 \pi^4}{\phi^4}) + B_o D_2 (\frac{1}{80} \frac{m^4 \pi^4}{\phi^4} - \frac{1}{3} \frac{m^2 \pi^2}{\phi^2})$$

$$+ B_2 D_o (24 - 2 \frac{m^2 \pi^2}{\phi^2} + \frac{1}{80} \frac{m^4 \pi^4}{\phi^4}) + C_o C_2 (\frac{1}{80} \frac{m^4 \pi^4}{\phi^4} - \frac{m^2 \pi^2}{\phi^2}) + D_o D_2 (\frac{1}{12} \frac{m^4 \pi^4}{\phi^4} - 4 \frac{m^2 \pi^2}{\phi^2})]$$

$$- k_f \frac{m^2 \pi^4}{\phi^2} [(1 - \frac{\gamma}{2}) (\frac{1}{11264} + \frac{B_o}{2304} + \frac{B}{2304} + \frac{D_o}{448} + \frac{D_2}{448} + \frac{A_o A_2}{2304} + \frac{A_o C_2}{448}$$

$$+ \frac{A_2 C_o}{448} + \frac{B_o B_2}{448} + \frac{B_o D_2}{80} + \frac{B_2 D_o}{80} + \frac{C_o C_2}{80} + \frac{D_o D_2}{12}) - \gamma (\frac{A_o}{11264} + \frac{A_2}{11264} +$$

$$\frac{C_o}{2304} + \frac{C_2}{2304} + \frac{A_o B_2}{2304} + \frac{A_2 B_o}{2304} + \frac{A_2 D_o}{448} + \frac{A_o D_2}{448} + \frac{B_o C_2}{448} + \frac{B_2 C_o}{448} + \frac{C_o D_2}{80} + \frac{D_o C_2}{80})] \}.$$

TABLE 1

CONVERGENCE OF GALERKIN SERIES

Shape of Channel	Width of web b_w (in.)	Width of flange b_f (in.)	Elastic Modulus E (ksi)	Loading Condition γ	No. of Galerkin terms	Flange Buckling Constant k_f	Half wave length of Buckle λ (in.)	Flange-Stiffener Junction Condition
(1)	(2)	(3)	(4)	(5)	(6)	(7)	(8)	(9)
	7.96	3.02	34,000	0	1 2 3	0.7965 0.7896 0.7896	7.067 6.568 6.568	Elastically built in Eq. (28)
	8.11	3.00	30,500	1	1 2 3	0.7348 0.7344 0.7344	6.965 6.949 6.949	
	4.00	1.1825	27,743	0.5	1 2 3	1.129 1.128 1.128	3.156 3.155 3.156	Simply supported Eq. (24)
				2.0	1 2 3	1.141 1.139 1.139	3.146 3.136 3.136	

TABLE 2

FLANGE BUCKLING CONSTANTS FOR
CONCENTRICALLY LOADED STIFFENED CHANNELS

Channel Series No. (1)	Flange Thinness Ratio $b_{f/t}$ (2)	$\dfrac{k_f \text{ (based on Eq. (28))}}{k_f \text{ (based on Eq. (24))}}$ (3)
H	56.3	0.999
TOR	56.3	1.006*
D,E	56.6	1.011*
B	148.1	1.009*
MCM	148.1	1.009*
MCMC1	149.6	1.000
MCMC2,3	149.3	0.999
T1LL	155.0	1.006*
T2LL	155.0	1.004*
T3LL	149.1	1.004*
T4LL	149.1	1.003*
CSLL	83.6	0.996
G20CS1	80.3	0.993
G20CS2,3	80.3	0.996
G20TS1	79.8	1.003*
G20TS2	79.5	1.004*
G22CS1	90.4	0.996
G22CS2	90.7	0.972
G22CS3	90.1	0.995
G22TS1	89.8	1.003*
G22TS2	90.4	1.040*
G24CS1	118.9	0.993
G24CS2	118.1	0.997
G24CS3	118.1	0.996

* correspond to channels in which the sizes of edge
  stiffeners were slightly larger than the ones
  recommended in Refs. [1] and [7]

TABLE 3

FLANGE BUCKLING CONSTANTS FOR
ECCENTRICALLY LOADED STIFFENED CHANNELS

Channel Series No. (1)	Flange Thinness Ratio $b_{f/t}$ (2)	k_f (based on Eq. (28)) / k_f (based on Eq. (24)) (3)
G8SL	17.6	0.998
G10SL	22.4	0.999
G12SL1,2	27.6	0.998
G12SL3	27.5	0.997
G14SL1,2	39.2	0.997
G14SL3	39.2	0.995
G16LL1,2	47.7	0.999
G16LL3	47.7	1.000
G16LL4	48.2	0.999
G18LL1	59.0	0.999
G18LL2	59.8	1.000
G18LL3	59.4	1.000
G20LL1	75.1	0.994
G20LL2	75.1	0.993
G20LL3	75.1	0.996
G20LL4	74.9	0.995
G22LL	91.1	0.996
G24LL1	111.2	0.997
G24LL2,3	111.5	0.998
G26LL1	148.8	0.995
G26LL2	148.3	0.995
G26LL3	149.3	0.996
G28LL1	174.4	0.996
G28LL2	173.8	0.995
G28LL3	173.8	0.996
G30LL1	211.2	0.991
G30LL2	209.8	1.014
G30LL3	209.8	0.994
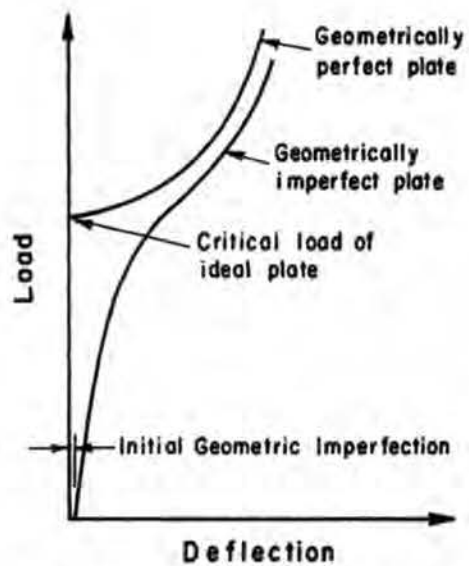
FIG. 1a – LOAD VERSUS DEFLECTION OF *GEOMETRICALLY PERFECT AND IMPERFECT PLATES IN COMPRESSION*
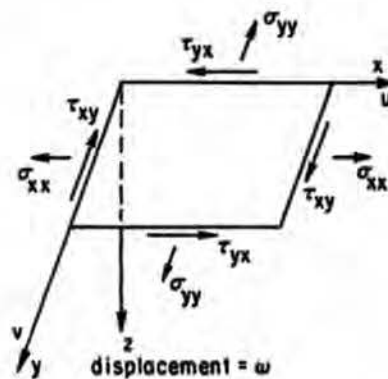
FIG. 1b – MIDDLE SURFACE FORCES AND DISPLACEMENTS OF A PLATE
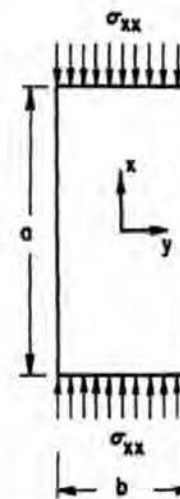
FIG. 1c – PLATE UNDER UNIAXIAL LOADING

(a) Loading Diagram

(b) Equivalent Loading Systems

(c) Free Body Diagrams of Web and Flange Plate Components
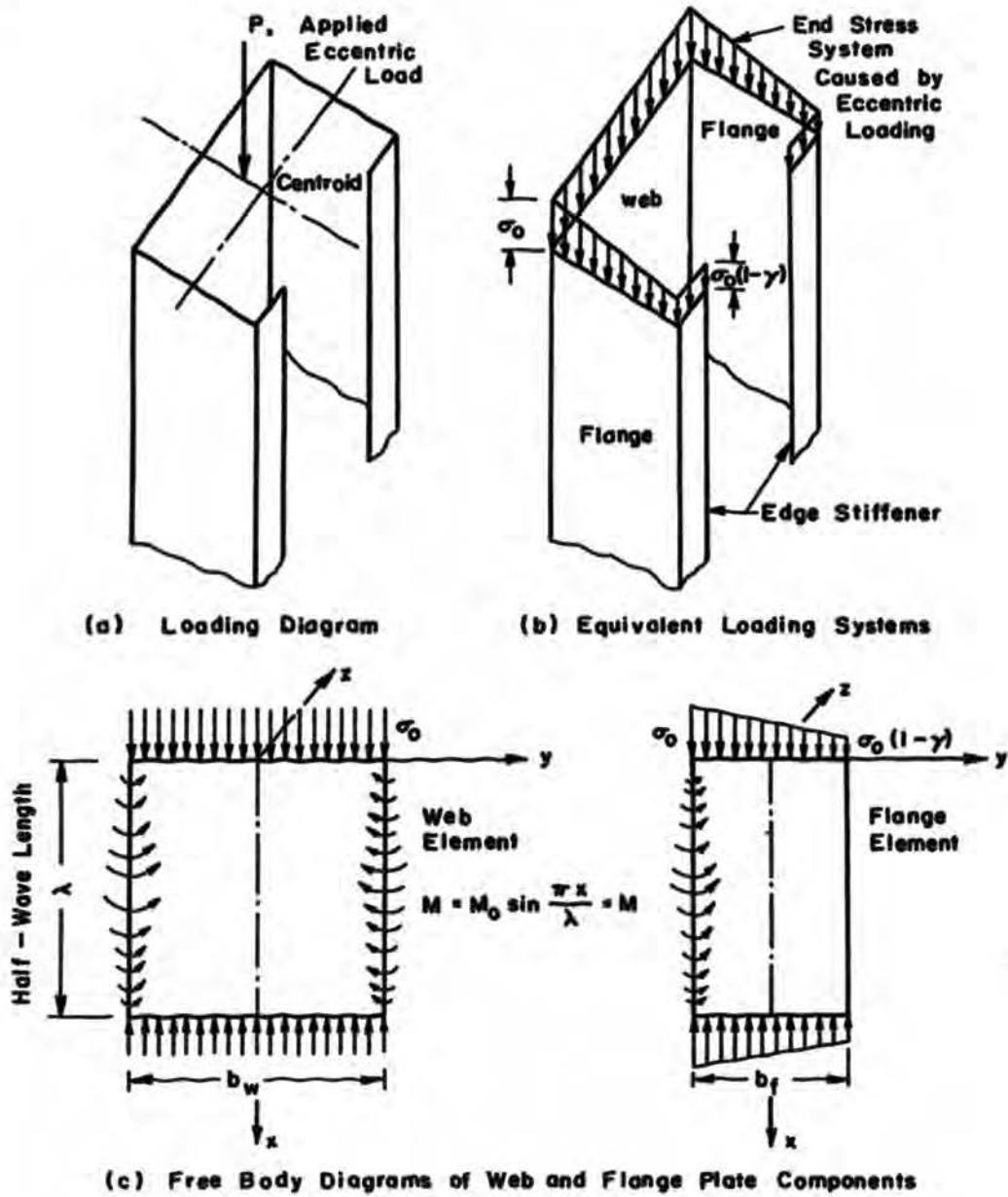
FIG. 2 — LOADING DIAGRAMS OF CHANNEL SECTION
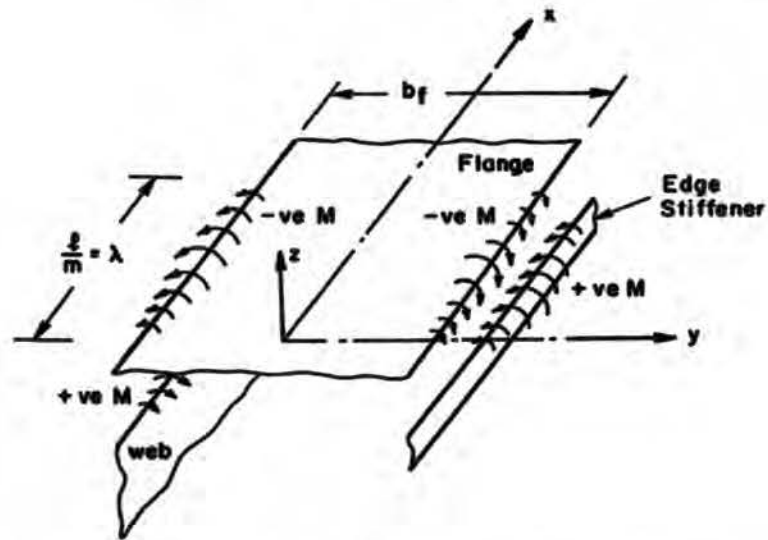
FIG. 3a — ELASTICALLY BUILD IN EDGE STIFFENER
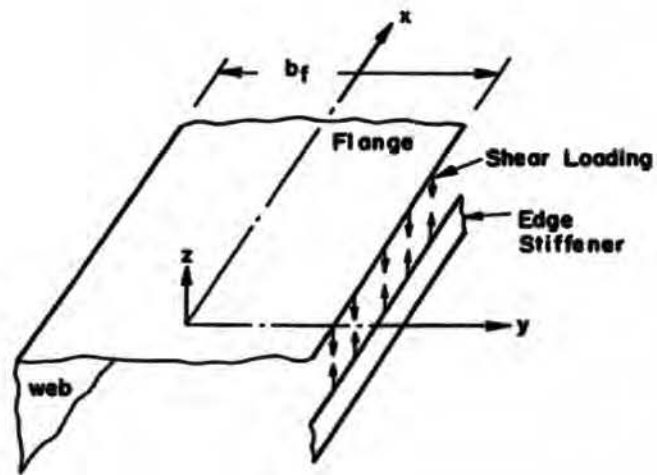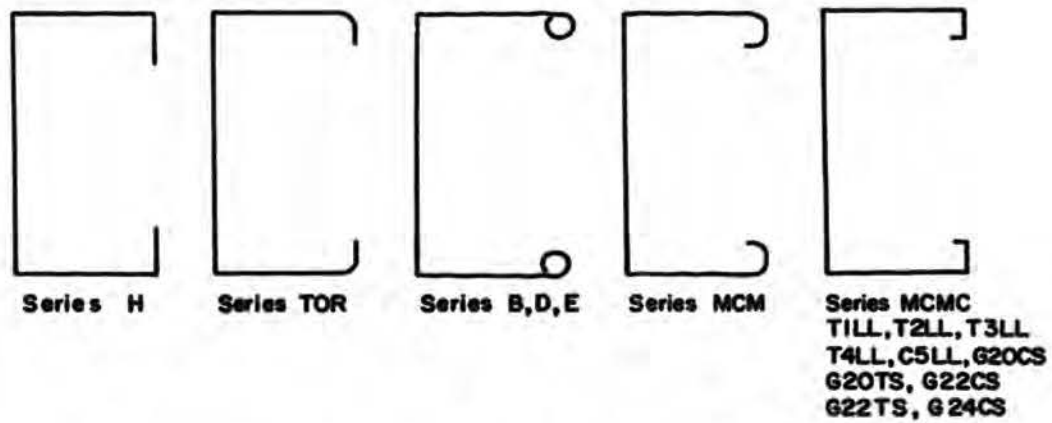

FIG. 3b — SHEAR LOADING AT FLANGE-STIFFENER JUNCTION

Series H   Series TOR   Series B,D,E   Series MCM   Series MCMC
TILL, T2LL, T3LL
T4LL, C5LL, G20CS
G20TS, G22CS
G22TS, G24CS

FIG. 4a — CONCENTRICALLY LOADED THIN-WALLED CHANNEL SHAPES

Straight-Lipped Channel
Series G8SL
G10SL
G12SL
G14SL

L - Lipped Channel
Series G16LL, G18LL
G20LL, G22LL
G24LL, G26LL
G28LL, G30LL
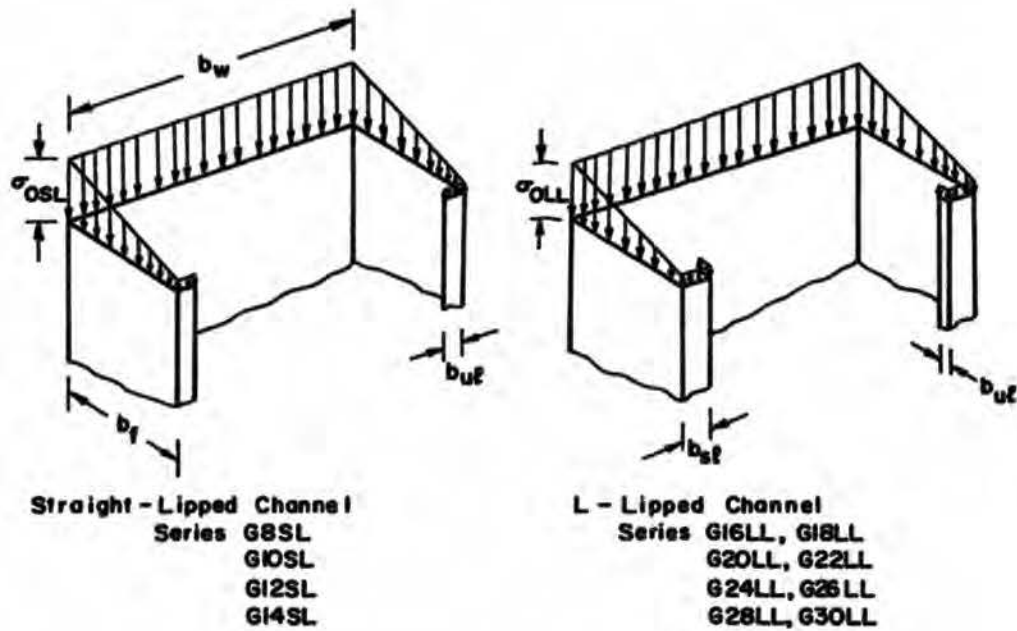
FIG. 4b — ECCENTRICALLY LOADED THIN-WALLED CHANNEL SHAPES
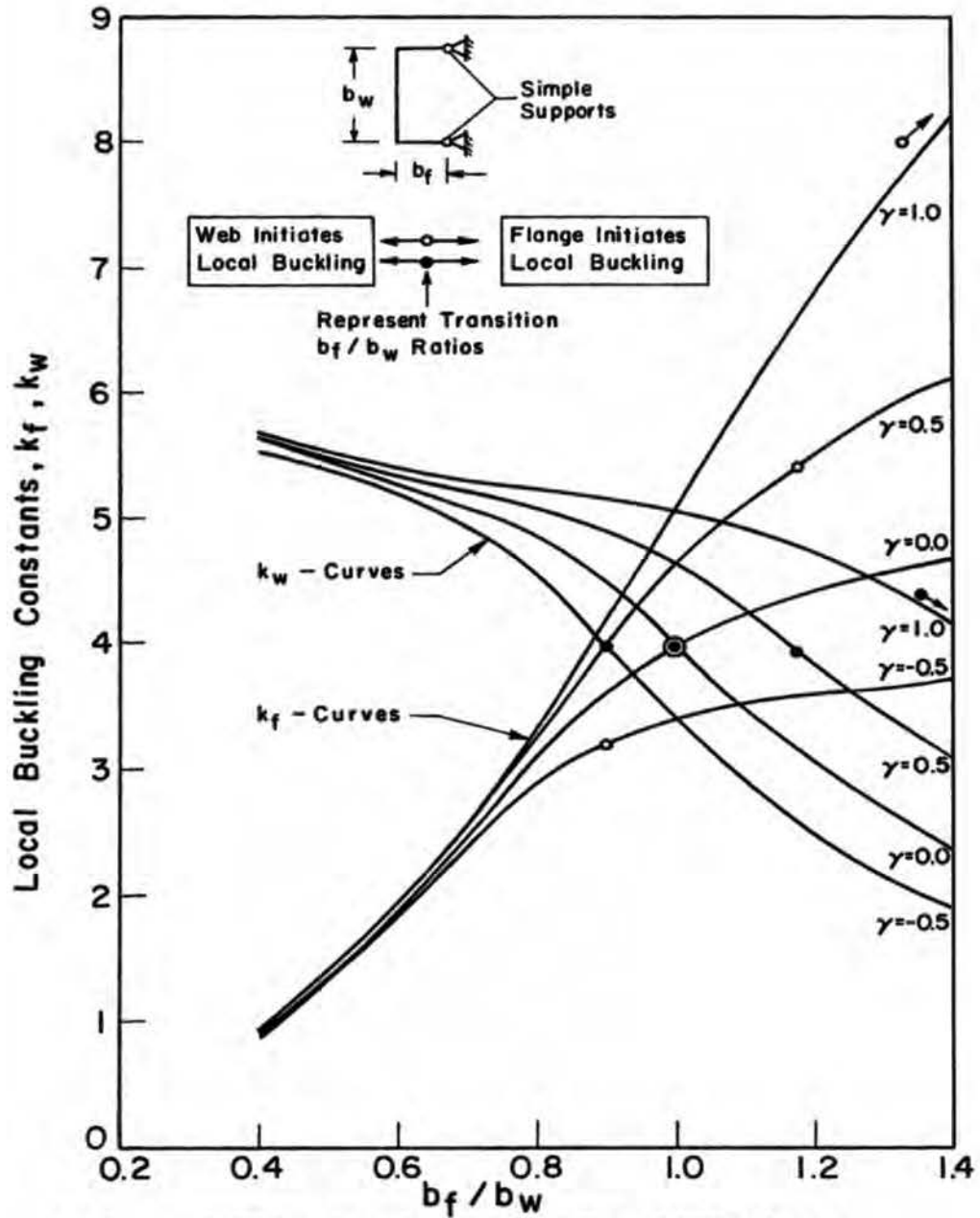
FIG. 5 – VARIATION OF LOCAL BUCKLING CONSTANTS
WITH GEOMETRY FOR CHANNEL SECTIONS
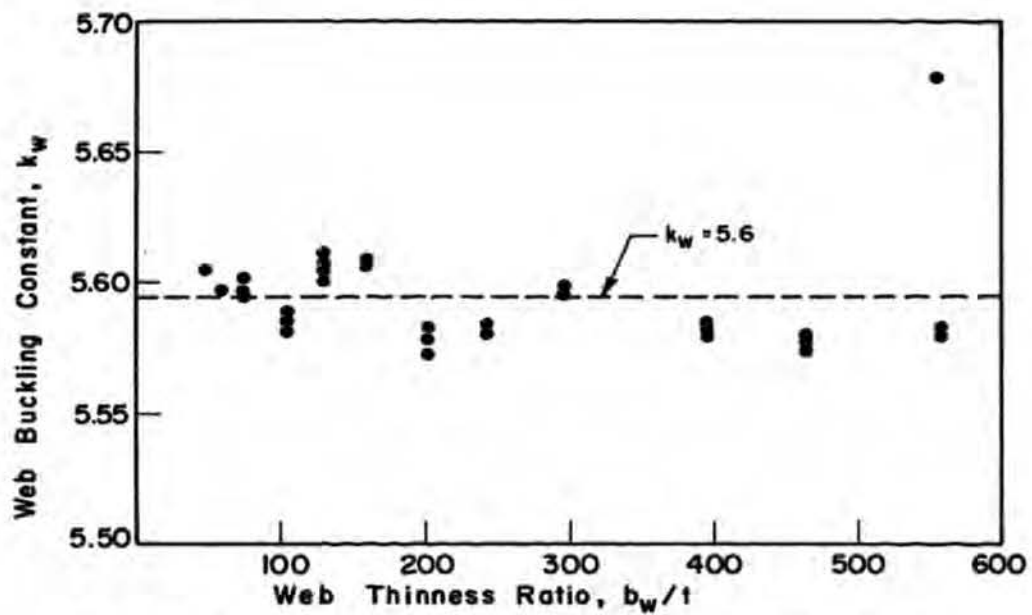
FIG. 6 – BUCKLING CONSTANT OF A UNIFORMLY COMPRESSED PLATE
ELASTICALLY RESTRAINED ON BOTH UNLOADED EDGES
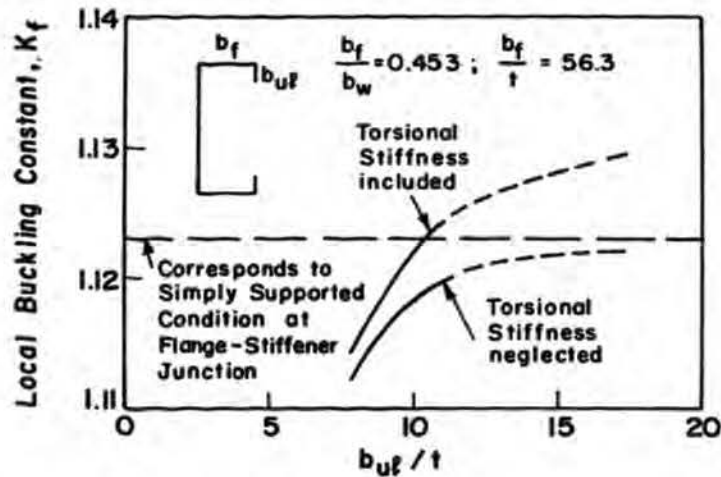
FIG. 7 — EFFECT OF TORSIONAL STIFFENESS OF STRAIGHT-LIP EDGE
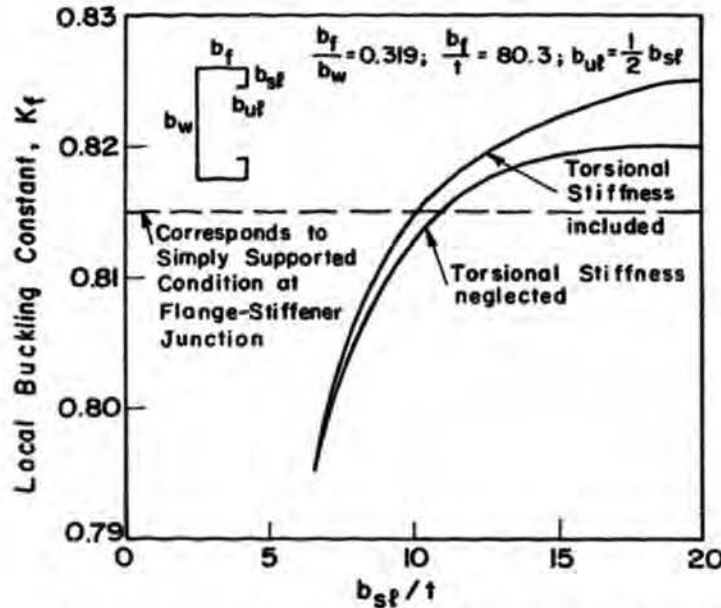STIFFENER ON LOCAL BUCKLING CONSTANT (CONCENTRIC LOAD)

FIG.8 — EFFECT OF TORSIONAL STIFFNESS OF L-LIP EDGE STIFFENER
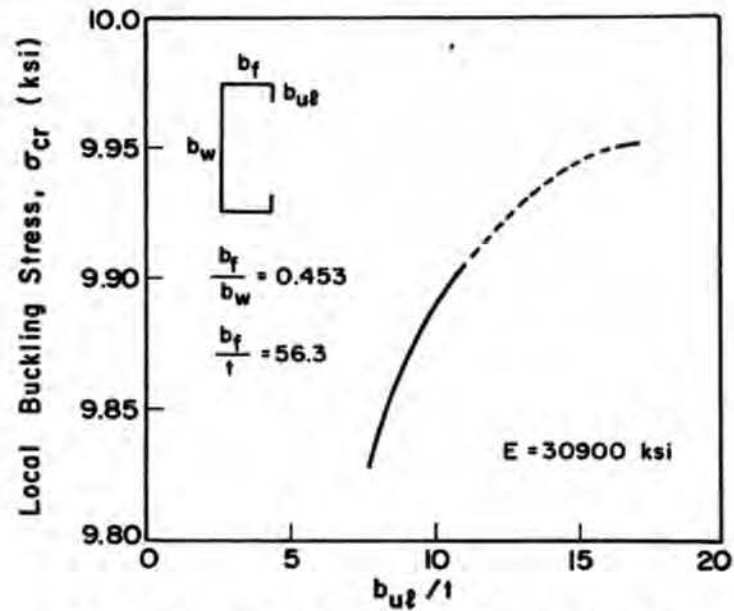ON LOCAL BUCKLING CONSTANT (CONCENTRIC LOAD)

FIG. 9 — VARIATION OF CRITICAL STRESS WITH SIZE OF STRAIGHT – LIP
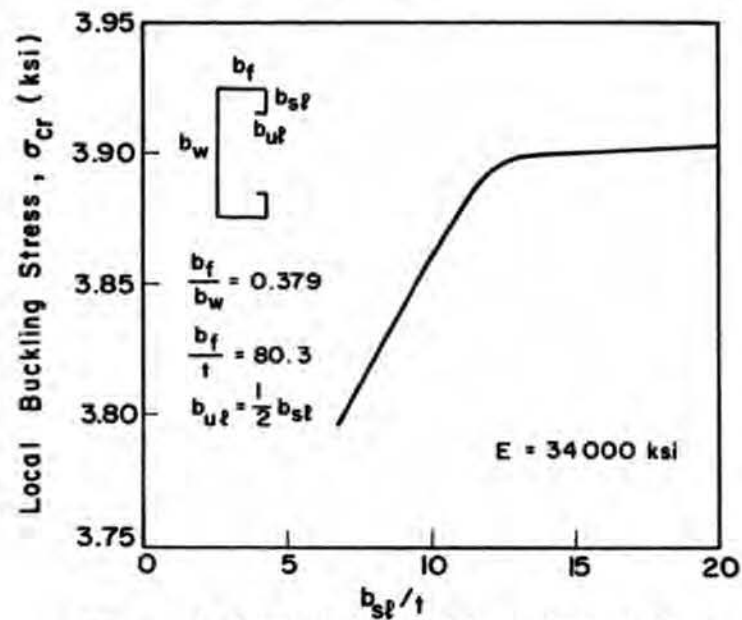

FIG. 10 — VARIATION OF CRITICAL STRESS WITH SIZE OF L – LIP